CIVE 693 – Candidacy Exam Proposal

CO_2 INJECTED 3D CONCRETE PRINTING: MULTISCALE CHARACTERIZATION

UNIVERSITY OF VICTORIA

By
Chirag Vijay Kumar

Supervisors:

Dr. Rishi Gupta

Dr. Bosco Yu

Contents

Introduction & Background

Concrete is everywhere—roads, buildings, bridges—but making it releases a lot of carbon dioxide (CO_2). Reviews of the cement and concrete sector estimate that cement production alone contributes on the order of eight percent of global CO_2 emissions, which is why researchers are exploring ways to turn concrete from a source of emissions into part of the solution. One promising idea is to store CO_2 inside the concrete itself while it is still fresh. Under the right CO_2 level, humidity, and exposure time, early-age carbonation turns some of the cement's hydration products into stable calcium carbonate minerals. This typically tightens the pore structure, speeds up early hardening, and reduces how easily water and salts move through the material, while locking carbon in place . In plain terms: we let the fresh material "breathe in" a controlled dose of CO_2 so it mineralizes and becomes denser. (Chen et al., 2023; Kazemian & Shafei, 2023; G. H. Kim & Yang, 2025; Meesaraganda & Kazmi, 2025; Misyura & Donskoy, 2020; Monkman et al., 2016a; Possan et al., 2016; Sodeifian et al., 2025; W. C. Wang et al., 2024; Zhu et al., 2024)

3D concrete printing (3DCP) makes this approach especially attractive. A printer lays down soft "beads" of concrete in layers, creating many fresh surfaces and interfaces between layers. Those interfaces often act as the weak link; printed versions of the same mix can be 12–22% lower in compressive strength than cast specimens because of interlayer weaknesses. Improving the bond between layers—and doing so without harming the fresh beads—is therefore central to reliable printed parts. (L. Li et al., 2023a; Tay et al., 2023)

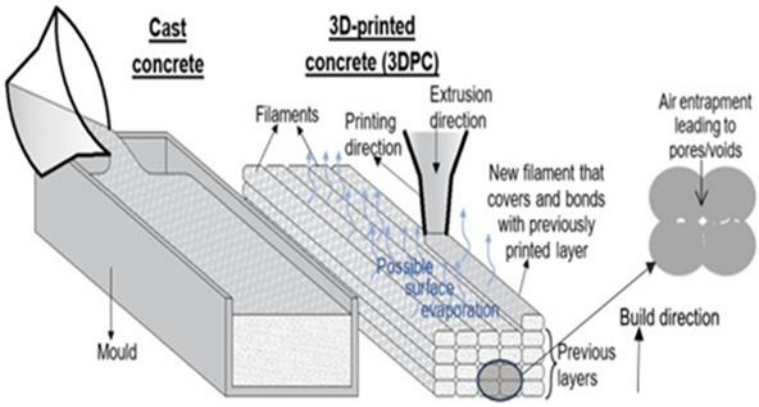

Figure 1: Picture showing cast concreting and 3D Printing

Workability vs. buildability. In traditional, cast-in-place concrete, accelerated carbonation can cut "open time" and reduce slump, making placement and finishing harder; in other words, early stiffening can be a workability penalty for ready-mix workflows. By contrast, 3DCP benefits from controlled early stiffening: higher early stiffness and yield stress improve shape retention and layer stability when they are timed to the layer cadence. The literature consistently reports early strength gains and lower absorption/chloride transport when exposure is well managed, but also warns that over-carbonation or poor environmental control can embrittle surfaces or weaken layer interfaces—exactly what we aim to avoid in printing(Driver et al., 2024; Han et al., 2025; Kmentová et al., 2025; Lee et al., 2025; Pivezhani et al., 2016; Qu et al., 2025; D. Wang et al., 2023a, 2023b; Zajac et al., 2022) . Several implementation pathways show the trade-offs. In post-printing chamber curing, exposing freshly printed parts to controlled CO_2 levels tightened pore structure and improved interlayer bonding in mixes with recycled constituents; for example, CO_2 curing reduced plastic shrinkage and increased both compressive and interlayer shear strength in printed mortars with recycled fine aggregate. Direct in-mix injection shows early-age strength benefits at modest doses by forming micro-scale calcium carbonate in paste voids. Jetting CO_2 at the filament during deposition can raise uptake but risks disturbing the bead and reducing layer bond unless moisture and temperature are carefully controlled. (*Exploring Carbon Sequestration Potential through 3D Concrete Printing (1)*, n.d.; Seifu et al., 2023; Tay et al., 2023)

This proposal takes a practical, test-what-you-claim approach. First, we will define safe operating windows for CO_2 dose and contact time that avoid overheating or surface damage. Next, we will test whether those settings measurably improve print quality (stable bead shape and stack height), interlayer bond, and early stiffness. Finally, we will scale to a small, printed element and count carbon fairly: stored CO_2 is only credited if the element also passes basic performance checks (geometry, bond, and a quick durability). In short, our aim is to turn a high-emitting material into a verified carbon store—and to show, with measurements rather than assumptions, where the carbon goes, how much stays, and whether the

printed element performs like good concrete should. (Jiang et al., 2025; Kaliyavaradhan et al., 2020; Karulf et al., 2025; L. Li et al., 2023b, 2023a, 2023c; Wen et al., 2021; Zhong et al., 2024)

Literature Review

The literature on CO_2 utilization in cementitious systems is broad and inconsistent in how exposure, humidity and timing are collected. Table 1 complies the routes most relevant to 3D concrete printing(3DCP) system level mineralization, introduction system, early age curing, reactive surface treatments, RCA carbonation, and SCM-rich binders. So, we can compare typical settings, what they achieve, and where they fail. The right-hand column is intentionally pragmatic: it states why each route matters for 3DCP, i.e., whether it helps printability (shape retention, stack height), interlayer bond, or durability. Read the table as a design space rather than a scoreboard; the next sections extract the gaps this comparison reveals and translate them into research questions that drive the proposed work.

Table 1. Evidence for CO_2 utilization routes relevant to 3D concrete printing (3DCP)

Focus	Sources	Typical CO_2 setting / uptake	Observations	Key risks & controls	Why this matters for 3DCP
System-level accelerated carbonation & mineralization	(Kashef-Haghighi & Ghoshal, 2013; Monkman et al., 2016b; Zhu et al., 2024)	Broad bands reported: 5–150 kg/m³ or 5–25% of binder, depending on method and mix.	Early-age strength ↑ (often +10–30%), pore refinement, permeability ↓, chloride transport ↓ when RH and CO_2 are controlled.	Over-carbonation → microcracks/shallow fronts; standardize dose–time–RH/T and QA logs.	Establishes credible result bands and the need for schedule-aware exposure and verification.
Ready-mix / inline direct injection (CRC)	(N. Kim et al., 2023; Possan et al., 2016; Zhang, 2024)	Injection within ~15–30 min of batching; ~8–15 kg CO_2/m³ stored (field-representative).	Early strength +10–20%; ITZ densification; sometimes lower water demand.	Plant timing & admixture interactions; enforce mixer/inline QA.	Translates to site logistics; informs same-schedule LCA assumptions.
Early-age chamber curing (post-print)	(X. S. Li et al., 2023; Quah et al., 2023; Seifu et al., 2023; D. Wang et al., 2023b)	~10–15% CO_2, ~60–70% RH, 12–36 h typical.	ITZ tightening; permeability/absorption ↓; early strength ↑.	Over-exposure → surface hardening or pore blocking; control RH/T.	Clean fit for 3DCP via tent/chamber over print envelope; improves buildability and interlayer bond.
Reactive surface carbonation (thin coatings)	(Hao et al., 2022; Lee et al., 2025; Misyura & Donskoy, 2020; Peng et al., 2023; B. Sun et al., 2022; Xiong et al., 2024)	Minutes-scale conversion of reactive film.	Capillary absorption ↓; pull-off bond ↑.	Specify film thickness, RH, cure time.	Fast protective finish for printed façades / marine exposures.
Recycled concrete aggregate (RCA) accelerated carbonation	(Sousanabadi Farahani et al., 2025; Wu et al., 2025; Zou et al., 2021)	Uptake in residual paste of RCA; depends on moisture/size class.	Concrete with carbonated RCA: strength +10–25%; absorption –20–40%.	“Shell-only” carbonation if moisture control is poor.	Stiffer, less-absorptive mixes stabilize extrusion rheology and interlayer bonding without excess paste.
Ternary SCMs (metakaolin + limestone)	(Schöler et al., 2017)	Reported binder-mass uptake bands; carboaluminate formation.	Early strength ↑; sulfate resistance ↑ via carboaluminates.	Tune MK/LS fractions, CO_2%, RH to avoid decalcification.	Low-clinker route that responds positively to controlled CO_2 for printable elements.
High-slag binders (GGBFS)	(Alonso-Cañon et al., 2025; Ashraf & Olek, 2018; Baghi et al., 2024; Kaliyavaradhan et al., 2020)	Moderate %CO_2; hours-to-days exposure windows.	~+30% early strength; pore mode shifts to 10–50 nm.	Over-exposure (>7 d) risks decalcification.	Fast-turnaround precast/printed modules without steam.

Focus	Sources	Typical CO_2 setting / uptake	Observations	Key risks & controls	Why this matters for 3DCP
3DCP with recycled fines (post-print CO_2)	(Ding et al., 2020; Lee et al., 2025; B. Sun et al., 2022)	Gentle chamber curing after deposition.	Plastic shrinkage ↓; compressive & interlayer shear ↑.	Avoid filament disturbance; control RH/T.	Direct evidence that post-print CO_2 can stabilize layers and boost bond.
UHPC under CO_2	(Briki et al., 2021; Kaliyavaradhan et al., 2020; Kmentová et al., 2025; Q. Liu et al., 2024; Schöler et al., 2017; Wen et al., 2021; Zajac et al., 2022)	Shallow fronts in very dense matrices.	Small early compressive ↑; near-surface pores refined.	Limited storage (depth-limited).	Use for surface-level upgrades; not a storage workhorse.
Alkali-activated materials (AAMs)	(Amran et al., 2022; Bawab et al., 2025; J. Sun et al., 2025)	Chemistry-dependent; prefer Ca-rich systems.	Ca-rich: permeability ↓ with acceptable strength; low-Ca FA: risk of gel depolymerization/pH drop.	Keep mild CO_2 and conservative windows; verify before use.	Targeted use only; protect long-term alkalinity & steel passivation.

Abbreviations: RH = relative humidity; ITZ = interfacial transition zone; FA = fly ash; MK = metakaolin; LS = limestone powder; UHPC = ultra-high-performance concrete; CRC = carbonation-ready concrete.

Table 1 puts together the main CO_2-utilization routes (system-level mineralization, ready-mix/inline injection, early-age chamber curing, reactive surface coatings, RCA carbonation, SCM-rich binders, UHPC, and AAMs) and distills what they typically achieve, where they can fail, and why they fit 3D concrete printing (3DCP). Across the board, controlled carbonation converts part of the cement's hydration products especially calcium hydroxide and portions of C-S-H into stable calcium carbonate, which tightens pores and can increase early stiffness/strength when humidity, CO_2 level, and time are set correctly. Typical ranges and what they mean: As mixes and test methods differ, reported CO_2 uptake spans single-digit to >100 kg/m³ and early-age strength gains are often ~10–30% under ~10–20% CO_2 and ~60–70% RH bands echoed across reviews and experimental studies cited in the table. These improvements track with pore-size refinement (toward ~10–50 nm) and lower sorptivity/chloride transport signals linked to better durability. **Why 3DCP especially benefits:** For cast-in-place concrete, accelerated carbonation can shorten open time and reduce slump, which hurts workability. In 3DCP, the same controlled early stiffening is an asset: it improves shape retention and layer stability when timed to the layer cadence, and it can strengthen the interlayer bond—the usual weak point in printed parts. The post-print chamber pathway in Table 1 aligns naturally with printing (tent/chamber over the print envelope), while inline/ready-mix dosing informs batch logistics and same-schedule LCA.

Identification of Research Gaps from Table 1:

- **CO_2 Introduction Window**: System-level mineralization gives the broadest result bands (uptake and early strength) but also the widest variability hence the need to regulate correct dose–time–RH/temperature and QA logs when moving from lab to practice.
- **Admixture interaction uncharacterised:** Ready-mix/inline injection shows ~8–15 kg/m³ stored and +10–20% early strength when metered ~15–30 min after batching; plant timing and admixture interactions are the key controls.
- **Interlayer-Bond under measured:** Early-age chamber curing (~10–15% CO_2; ~60–70% RH; 12–36 h) tightens the ITZ and reduces permeability—useful for buildability and interlayer bond in 3DCP.
- **Reactive coating and carbonated recycled concrete aggregate:** Reactive coatings carbonate within minutes and lower capillary absorption while raising pull-off bond—a fast finish for façades or marine exposure. RCA carbonation upgrades aggregate (less absorption, harder surface) and improves concrete strength by ~10–25% when moisture/size are controlled; for 3DCP, this stabilizes extrusion rheology and interlayer bonding without excess paste.
- **Supplementary Cementitious Materials (SCMs) not tuned to printing:** SCM-rich binders (slag-rich; MK + limestone ternaries) show synergy under controlled CO_2: ~30% 3-day strength in

high-slag systems and carboaluminate formation in MK+LS, with pore-mode shifts into the fine range good news for low-clinker printable binders.

- **Dense mixes store CO_2 only near the surface:** UHPC benefits are surface-limited (dense matrix), so use it as a surface upgrade, not as a storage workhorse.
- **Alkali-Activated Materials (AAMs):** AAMs are chemistry-dependent: Ca-rich (slag) can gain; low-Ca/high-FA can suffer gel depolymerization and pH drop if pushed so keep mild CO_2 and conservative windows, verified before adoption.
- **Element-Level Proof of Performance:** Most work stops at paste/mortar scale. We will test a printed element and grant any CO_2 credit only if all performance criteria are acceptable.

Risks and why controls matter: -

Based on the literature review, currently every methodology that has been conducted as led to failure when exposure to CO_2 exceeds a safe window. Too much CO_2 causes micro cracks, shallow fronts and blocked pores that reduce durability and layer bond. We must limit the temperature to a certain acceptable limit and so do these also RH and log every trials.

Mechanisms and pathways background for Table 1

1. Chemically, accelerated carbonation/mineralization targets portlandite and parts of C-S-H to form $CaCO_3$, densifying the microstructure and typically increasing early stiffness/strength when RH (~60–70%), CO_2 (~10–20%), and time are tuned to the mixture. Reported uptake ranges run from single digit to >100 kg/m³, explaining the spread seen in Table 1's cells.
2. Process routes for 3DCP mirror Table 1: (i) direct injection to fresh mix/line (~15–30 min window; ~8–15 kg/m³ stored), (ii) early-age chamber after deposition (~10–15% CO_2; 12–36 h), and (iii) reactive coatings as a rapid finish. Each enhances different parts of the system batch logistics, interlayer zone, or surface durability.
3. Performance and durability: Studies report ~15–30% early-age strength gains (24–48 h), pore refinement to ~10–50 nm, and measurable drops in sorptivity and chloride migration with the bonus that carbonation depth in dense matrices is usually shallow, preserving core hydration.
4. SCM synergy and circular materials: Fly ash, high-slag, and MK+LS ternaries respond well under controlled CO_2, delivering faster early gains and better transport resistance; RCA carbonation upgrades aggregate to help buildability in prints.
5. AAMs: Useful but not universal Ca-rich systems tolerate moderate CO_2; low-Ca mixes need caution to protect long-term alkalinity and steel passivation.
6. Standards and verification: The literature repeatedly calls for harmonized uptake methods (mass-gain/TGA), depth, and permeability benchmarks, plus clear code pathways exactly the kind of audit trail your study proposes to provide.

Summary of gaps and novelty of proposed study

1. Process control vs. real printing. Most studies ran chambers or small molds without tying dose/contact to layer cadence/open time/stack height; **Novelty: synchronize exposure to printing**.
2. Interlayer bond is under-measured. Many papers report compressive strength/durability but lack direct tension or slant-shear across printed interfaces; **Novelty: elevate interlayer bond to a primary metric.**
3. Geometry and stability rarely gated. Few enforce "did it print correctly?" checks (±10% bead/wall, stable stack); **Novelty: add printability acceptance criteria**.
4. Thermal/RH not actively managed. Exposure windows often ignored temperature/moisture limits; **Novelty: use IR + RH control and abort criteria**.
5. Uptake claims without performance proof. Some credit stored CO_2 without verifying structural/durability targets; **Novelty: adopt "no pass → no credit" in LCA**.
6. Lab results not promoted to elements. Many stops at pastes/mortars; **Novelty: test a small, printed element and only count carbon for a passing element.**
7. Standards/audit trail missing. Reporting of methods/logs is inconsistent; **Novelty: build a full audit trail (schedule, geometry, properties, carbon) mapped to referenced test methods**.

Research Questions

- RQ1 — Carbon-dioxide setting. What dose (as a percentage of binder mass) and what contact timing produce early mineralization without harmful temperature rise or surface chalking?

- RQ2 — Printability and interlayer bond. Under those settings, can bead and wall geometry remain within tolerance, stacks remain stable, and layers bond strongly?
- RQ3 — Structural checks. When a small, printed element is made with the same settings, does it meet load and service criteria without failure along a weak layer?
- RQ4 — Carbon impact under the same schedule. Does the net global-warming potential decrease when carbon credit is granted only after all acceptance criteria are passed?

Expected contributions (what this study adds)

- Method → not numbers- A repeatable method to find the right carbon-dioxide setting for *any* mix: small pilot matrix (dose × contact time), temperature safety cap, and go/no-go rules. You tune it locally; the playbook stays the same.
- Printability envelope procedure - A simple way to map “can it print and hold shape?” using bead/wall checks now and at fifteen–thirty minutes, plus a stable-stack test. Outputs are pass/fail against a tolerance you set project-by-project.
- Interlayer bond protocol (normalized) -Pull-off and slant-shear across layers, always reported relative to the same-day control. Because it is normalized, the data travel across mixes and plants.
- Pass-gated carbon accounting - A credit-only-when-it-passes rule and a logging template (materials, energy, transport, waste, measured storage). Works with any supplier and any binder—no fixed recipe assumed.
- Acceptance checklist you can drop into specs - Plain language criteria (geometry within tolerance, stack height achieved, bond ≥ control, quick durability improved) that owners can put in tenders—with the tolerance value left blank for local choice.
- Standard data schema and forms - Ready-to-use sheets for dose, timing, printer speed, surface temperature, ambient, materials, energy, transport, waste, and lab results—so teams can audit and compare across jobs.
- Two mix-independent indices – (1) Interlayer Bond Index (IBI): bond of printed coupon ÷ bond of same-day cast/control. (2) CO_2 Uptake Index (CUI): measured stored CO_2 ÷ binder mass (or ÷ element volume) for passing prints only. Both are dimensionless and comparable across mixes.
- Risk controls and stop rules - A short list of abort conditions (temperature-rise cap, surface chalking, geometry drift beyond tolerance) that any crew can apply without changing a mix.
- Training and commissioning flow - A three-step onboarding for new plants: (1) calibration matrix, (2) printability and bond gate, (3) one element and pass-gated carbon. This reduces trial-and-error regardless of the recipe.

Research Proposal

Objectives:

Micro — Material & Microstructure

- Map the pore structure with Scanning Electron Microscopy and quantify pore size distribution and total porosity.
- Link pore structure metrics to durability indicators such as absorption and chloride transport.
- Build a simple early-age strength model for zero to seventy-three hours using Ultrasonic Pulse Velocity and confirm mineral formation with spectroscopy and thermogravimetry.

Meso — Process & Interface

- Prove clean printing: stable bead and wall geometry and a stack that holds its shape.
- Measure the interlayer bond under direct tension and under slant-shear and compare against the control.
- Control temperature rise during mixing and printing to avoid surface chalking and thermal cracking.
- Document the full printing window: layer timing, contact time, and environmental conditions.

Macro — Structural Performance

- Test a printed element (panel or beam) for load and service behaviour and confirm failure is not along a weak layer.
- Evaluate long-life behaviour under small, repeated load cycles.

- Check response to lateral actions: low-cycle bending or seismic-type loading, and wind-induced comfort effects where relevant.
- Assess fire performance of printed elements with a simple thermal exposure and residual-strength check.
- Investigate reinforcing-bar bond in printed material with a pull-out test.
- Trial overlays and jacketing as retrofit strategies on printed substrates and measure interface strength.

Experimental Methodology

Overview

This study advances in three stages that move from material behaviour to process behaviour and finally to element-scale verification. The goal is to show that early-age, printing-aware exposure to carbon dioxide can permanently store carbon while preserving or improving printed quality. A common operating window is enforced across all stages: the carbon-dioxide dose is selected in three bands (low, mid, and high as a percentage of binder mass), contact is applied for defined durations beginning at the start of mixing or at clearly defined moments during deposition, and the environment is held within a controlled range of relative humidity and ambient temperature—ranges consistent with accelerated carbonation curing practice . An infrared camera continuously records surface temperature; any schedule is aborted if the temperature rise exceeds a pre-set cap or if a chalky skin appears. Replication is built in by testing multiple specimens of each type, and every schedule will be compared to two same-day controls: a cast control and a printable control with no carbon-dioxide exposure.

Phase One: Micro (material and microstructure)

The objective is to **lock a printable base mixture** and to **identify safe, effective windows of dose and contact time** that increase early stiffness and form measurable calcium carbonate without surface damage. The mixture uses **a fixed water-to-binder ratio, a defined sand grading, and a standard combination of superplasticizer and viscosity modifier**. **Four batches are made: a control with no carbon-dioxide exposure and three levels with in-mix dry-ice dosing**. Early behaviour over the first six hours is tracked by **recording Ultrasonic Pulse Velocity at regular intervals and converting those readings into a relative stiffness scale**; **a vane or needle check records the time at which the paste shows no visible slump**. **Infrared temperature is recorded throughout, and any overshoot above the temperature-rise cap triggers an immediate stop**. To confirm mineral formation, **paste samples are tested by Attenuated Total Reflectance–Infrared Spectroscopy and by Thermogravimetric Analysis at approximately two hours and again at twenty-four hours**. To gauge whether transport pathways are tightening, **small prisms are tested using water absorption or a short-duration Rapid Chloride Permeability surrogate**. This “mechanism-plus-performance” approach follows established carbonation-curing protocols (Lu et al., 2024; Osman et al., 2021; Zajac et al., 2022; Zhu et al., 2024) .

Phase Two: Meso (process and interface)

The aim is to show that **the same windows of dose and timing produce clean printing and strong interfaces between layers**. **A SCARA operating at a specified speed and nozzle diameter lays down straight beads and short walls for each schedule that passed the Micro stage**. **Bead width and height and wall height are measured immediately after placement and again after fifteen to thirty minutes to evaluate geometric stability during the open-time window**; **walls are then built to the maximum height that can be stably stacked, and any failure is logged as buckle, slide, or collapse**. **Interlayer bond is quantified on coupons cut across layer interfaces using direct-tension pull-off and slant-shear tests at defined angles**; **for each schedule, the mean value, the standard deviation, and the ratio to the printable control are reported**. The environmental window is maintained, and the infrared camera continues to enforce the temperature cap. The selected measurements and acceptance logic are aligned with reports on post-print chamber curing and interface strengthening in printed mortars, including those with recycled fines. ***The Ultrasonic Pulse Velocity–based early-age strength model is used here to select layer-to-layer timing and to verify that printing windows chosen in practice align with the predicted strength and stiffness gain.***

Field validation using the SCARA Road Runner. **The same in-mix carbon-dioxide method will be verified on the SCARA printer**. **Targets are bead width and wall height within ten percent of target; a full, time-stamped log of carbon-dioxide dose, contact timing, printer revolutions per minute, surface temperature, and ambient conditions**. **One baseline print with no carbon-dioxide**

and two carbon-dioxide schedules will be run. Specimens include one single-pass line and one multi-layer wall; cut samples are returned for layer-bond and mineralization checks. The field sequence is print line → print wall → verify size and height (ten percent tolerance) → cut samples → export the complete log for the life-cycle assessment. (Chandra Kishen et al., n.d.; Curth et al., 2024; Davolio et al., 2025; Fetzer et al., 2025; Kashef-Haghighi & Ghoshal, 2013; Khan & Koç, 2023; Kristombu Baduge et al., 2021; Krstulovic & Dabic, n.d.; Lachmayer et al., n.d.; Quah et al., 2023; Rymeš et al., 2024; Tarhan & Şahin, n.d.; Wolfs & Suiker, 2019; Žitek Makoter et al., 2025)

Phase Three: Macro (element-level proof and fair carbon accounting)

A single small element—a panel or beam printed with the same settings that passed the Meso stage—is tested with engineering methods to confirm structural adequacy and to compute net carbon fairly. **The element is loaded in four-point bending, or in compression where appropriate, while load versus deflection is recorded and a crack map is kept; the failure mode is checked to ensure it is not governed by a weak layer**. **Specimens are cut from the printed element to repeat the same quick durability used earlier (absorption or short-duration RCPT)**. **A fair carbon balance is then performed:** net global-warming potential **equals materials plus mixing, pumping, and printing energy plus transport, minus measured mineralized CO_2 obtained from spectroscopy and thermogravimetry on samples from the element**. **Carbon credit is reported only if the element meets the geometric, interlayer-bond, and durability criterias**. This sequencing follows the literature emphasis on chamber control, deployment practice, and verification before crediting carbon storage . Life-cycle assessment scenarios. **Results are reported for three scenarios: S0 (cast, no carbon-dioxide), S1 (cast, in-mix carbon-dioxide), and S2 (three-dimensional-printed, in-mix carbon-dioxide). For each scenario we compute Net global-warming potential = materials + mixing, pumping, and printing energy + transport − measured stored carbon-dioxide, and we show the percent change relative to S0 with a small uncertainty bar. Acceptance conditions for carbon credit. Carbon credit will be reported only when all of the following are satisfied by the printed element made with the same schedule: (1) bead width and wall height are within the defined geometry tolerance; (2) the wall stack reaches its target height without failure; (3) the interlayer bond is equal to or greater than the printable control; (4) water absorption is lower than the control; (5) the rapid chloride permeability (short-duration surrogate) is lower than the control; (6) the carbonation depth meets the project's limit for the selected exposure class; and (7) Attenuated Total Reflectance–Infrared Spectroscopy shows a carbonate signal at or above the set threshold for acceptance.** (Davolio et al., 2025; Jin et al., 2025; Kazemian & Shafei, 2023; N. Kim et al., 2023; B. Liu et al., 2021; Pan et al., 2023; J. Sun et al., 2021)

(Net global-warming potential = materials + mixing, pumping, and printing energy + transport and waste − measured stored carbon-dioxide.)

Analysis and Modelling of Results

Interpreting the Micro stage:

Ultrasonic Pulse Velocity time-series will be converted into relative stiffness curves, and the no-slump timestamp will be extracted from the vane or needle check. Infrared temperature logs will be reviewed to verify that all data being analysed stayed at or below the temperature-rise cap; runs that exceeded the cap are excluded. Spectroscopy and thermogravimetry traces will be interpreted to confirm the presence of calcium-carbonate peaks or mass-loss signatures associated with carbonate formation. Scanning Electron Microscopy images will be taken at consistent magnification and field of view to avoid edge effects, and simple counts of void frequency and average void area will describe pore refinement. The quick durability indicator—absorption or short-RCPT—will be expressed as a percent change relative to the same-day control and plotted against the pore metrics to demonstrate that fewer and smaller pores coincide with lower transport. Advancement will require a smooth, increasing stiffness curve, confirmed carbonate formation, reduced transport relative to the control, and no temperature-cap violations—signals synthesised across accelerated-carbonation reviews.

Interpreting the Meso stage

Bead and wall measurements taken immediately after placement and again at fifteen to thirty minutes will be compared with their targets to quantify tolerance and to define a practical printability envelope that captures combinations of layer timing and bead stability that maintain geometry and permit stable stacking. Interlayer bond will be summarised as the mean and standard deviation for both pull-off and slant-shear, and each schedule will also be reported as a ratio to the printable control, so acceptance is

plain. The acceptance criteria are straightforward: geometry within plus or minus ten percent, stack height achieved without failure, and interlayer bond equal to or greater than the control with a preferred margin of ten percent; thermal safety will be documented by the peak temperature rise and the time spent at or above the cap. These outputs will also use to fit a two-parameter interlayer representation for the later parity check (tension intercept from pull-off; effective shear from slant-shear). Emphasis on geometric stability, stack ability, and interlayer performance will follow successful process- and interface-quality studies.

Interpreting the Macro stage.

The element test will be first checked for sensor artefacts or warm-up effects. The measured peak load and the service-level deflection will be compared with the target values, and the observed failure mode will be cross-checked against the two-parameter interlayer representation derived from the Meso stage; parity will be acceptable when the predicted failure locus matches the experiment and the predicted and measured peaks differ by no more than a practical ten percent band. The durability from the element will be compared with the same-day control using the same “lower is better” rule. The net global-warming potential will then be computed from material quantities, measured energy for mixing, pumping, and printing, transport distances, and the measured mineralized CO_2 from spectroscopy and thermogravimetry. Ninety-five percent confidence intervals will be displayed on the key plots—interlayer bond, geometry tolerance, and net global-warming potential—to communicate uncertainty. The decision rule is unchanged: a schedule passes only when every gate passes; only then is the carbon credit reported—consistent with pass-gated accounting recommended in reviews and deployment papers . After the Stage Three element passes all acceptance criteria , a short set of exploratory checks will be performed without delaying the primary deliverables. These checks probe risks highlighted in practice—low-cycle behaviour, wind comfort, fire exposure, reinforcing-bar bond, and retrofit overlays—using small, fast tests. Results will be reported as exploratory only; carbon accounting remains tied to the Stage Three pass.

Low-cycle loading (seismic): A small, printed specimen made with the same schedule is subjected to controlled load–unload cycles at increasing amplitudes. We will record hysteresis loops, stiffness reduction per cycle, residual deflection, and a crack map. The check is considered satisfactory when loops are stable within the planned range and no premature interlayer slip governs the response. ***Wind-comfort:*** For thin panel elements we apply a gentle, repeated lateral excitation (or its quasistatic equivalent) to observe drift, vibration comfort indicators, and any onset of serviceability issues such as rattling at interfaces. The check is considered satisfactory when measured deflection and response remain within the target comfort band and no interlayer distress is observed.

Thermal Exposure: Coupons sawn from the printed element mid-height are exposed to a defined temperature profile in a ventilated oven and then cooled to laboratory conditions. We will measure residual pull-off strength or residual compressive strength and document visible damage. The check is considered satisfactory when residual strength remains within the project’s target band and there is no interlayer delamination on visual inspection. ***Reinforcing-bar bond:*** Short prisms or cylinders printed with the same schedule will be cast or printed around a reinforcing bar that crosses layer interfaces. A monotonic pull-out test measures peak bond stress, slip at peak, and failure mode. The check is considered satisfactory when peak bond meets the target relative to the cast control and failure is not governed by a weak interlayer at service-level stress.

Retrofit overlay & jacketing: A thin overlay or jacketing layer is applied to a printed wall segment. After the specified cure, pull-off tests (and where appropriate, slant-shear tests) are performed through the overlay into the printed substrate. The check is considered satisfactory when overlay interface strength meets or exceeds the baseline, and failure occurs away from a weak interlayer plane. All specimens will use the same schedule that passed Stage Three (same dose, timing, and environmental controls). Test logs will include the loading or thermal profile, cycle counts or exposure time, specimen geometry, and any deviations. These validations will be scoped to be short and informative; if timing or resources constrain the work, they will be deferred without impacting the main claim.

References

Alonso-Cañon, S., Blanco-Fernandez, E., Cuesta-Astorga, E., Indacoechea-Vega, I., & Salas-Alvarez, J. (2025). Selection of the Best 3D Printing High-Performance Mortars Using Multi-Criteria Analysis. *Buildings*, *15*(18). https://doi.org/10.3390/buildings15183307

Amran, M., Abdelgader, H. S., Onaizi, A. M., Fediuk, R., Ozbakkaloglu, T., Rashid, R. S. M., & Murali, G. (2022). 3D-printable alkali-activated concretes for building applications: A critical review. In *Construction and Building Materials* (Vol. 319). Elsevier Ltd. https://doi.org/10.1016/j.conbuildmat.2021.126126

Ashraf, W., & Olek, J. (2018). Carbonation activated binders from pure calcium silicates: Reaction kinetics and performance controlling factors. *Cement and Concrete Composites*, *93*, 85–98. https://doi.org/10.1016/j.cemconcomp.2018.07.004

Baghi, A., Aminpour, N., Memari, A., Bilén, S., Nazarian, S., & Duarte, J. P. (2024). 3D concrete printing of self-supported filaments via entrained cables: constructing formwork-free spanning structures. *Virtual and Physical Prototyping*, *19*(1). https://doi.org/10.1080/17452759.2024.2379998

Bawab, J., El-Hassan, H., El-Dieb, A., & Khatib, J. (2025). Optimizing carbon sequestration and performance of concrete masonry blocks containing alkaline industrial waste. *Cleaner Engineering and Technology*, *26*. https://doi.org/10.1016/j.clet.2025.100943

Briki, Y., Zajac, M., Haha, M. Ben, & Scrivener, K. (2021). Impact of limestone fineness on cement hydration at early age. *Cement and Concrete Research*, *147*. https://doi.org/10.1016/j.cemconres.2021.106515

Chandra Kishen, J. M., Ramaswamy, A., Ray, S., Vidyasagar, R., Rymeš, J., Červenka, J., & Jendele, L. (n.d.). *MATERIAL MODELLING AND SIMULATION OF 3D CONCRETE PRINTING PROCESS*. www.cervenka.cz

Chen, X., Lv, L., Wu, Q., Cheng, S., Zhou, Q., Zhao, C., Fan, T., & Zhao, R. (2023). Optimization on the mix design method of self-compacting concrete with recycled coarse aggregate based on paste rheological threshold theory and material packing characteristics. *Construction and Building Materials*, *407*. https://doi.org/10.1016/j.conbuildmat.2023.133509

Curth, A., Pearl, N., Castro-Salazar, A., Mueller, C., & Sass, L. (2024). 3D printing earth: Local, circular material processing, fabrication methods, and Life Cycle Assessment. *Construction and Building Materials*, *421*. https://doi.org/10.1016/j.conbuildmat.2024.135714

Davolio, M., Muciaccia, G., & Ferrara, L. (2025). Concrete carbon mixing – A systematic review on the processes and their effects on the material performance. In *Cleaner Materials* (Vol. 15). Elsevier Ltd. https://doi.org/10.1016/j.clema.2025.100292

Ding, T., Xiao, J., Zou, S., & Wang, Y. (2020). Hardened properties of layered 3D printed concrete with recycled sand. *Cement and Concrete Composites*, *113*. https://doi.org/10.1016/j.cemconcomp.2020.103724

Driver, J. G., Bernard, E., Patrizio, P., Fennell, P. S., Scrivener, K., & Myers, R. J. (2024). Global decarbonization potential of CO2 mineralization in concrete materials. *Proceedings of the National Academy of Sciences of the United States of America*, *121*(29). https://doi.org/10.1073/pnas.2313475121

Exploring carbon sequestration potential through 3D concrete printing (1). (n.d.).

Fetzer, D. E. L., Coelho, J. A. P., & Ambye-Jensen, M. (2025). Extraction of lipids with supercritical CO2and downstream processing from grass-clover products from a green biorefinery demonstration platform. *Journal of CO2 Utilization*, *101*. https://doi.org/10.1016/j.jcou.2025.103198

Han, S., Kim, J. H., Singh, R. K., & Shah, S. P. (2025). CO2 utilization for cementitious materials - A review. In *KSCE Journal of Civil Engineering* (Vol. 29, Issue 4). Elsevier Inc. https://doi.org/10.1016/j.kscej.2025.100227

Hao, L., Xiao, J., Sun, J., Xia, B., & Cao, W. (2022). Thermal conductivity of 3D printed concrete with recycled fine aggregate composite phase change materials. *Journal of Cleaner Production*, *364*. https://doi.org/10.1016/j.jclepro.2022.132598

Jiang, P., Wang, F., Li, N., Wang, W., Wang, B., & Yu, P. (2025). Polyurethane foam lightweight concrete: Preparation, CO2fixation properties and mechanism. *Journal of CO2 Utilization*, *97*. https://doi.org/10.1016/j.jcou.2025.103109

Jin, P., Hasany, M., Kohestanian, M., & Mehrali, M. (2025). Micro/nano additives in 3D printing concrete. *Cement and Concrete Composites*, *155*. https://doi.org/10.1016/j.cemconcomp.2024.105799

Kaliyavaradhan, S. K., Ling, T. C., & Mo, K. H. (2020). CO2sequestration of fresh concrete slurry waste: Optimization of CO2uptake and feasible use as a potential cement binder. *Journal of CO2 Utilization*, *42*. https://doi.org/10.1016/j.jcou.2020.101330

Karulf, L., Singh, B., Singh, R., & Repo, T. (2025). Carbon dioxide utilization: CO2-based polyurethane foam. In *Journal of CO2 Utilization* (Vol. 91). Elsevier Ltd. https://doi.org/10.1016/j.jcou.2024.103000

Kashef-Haghighi, S., & Ghoshal, S. (2013). Physico-chemical processes limiting CO2 uptake in concrete during accelerated carbonation curing. *Industrial and Engineering Chemistry Research*, *52*(16), 5529–5537. https://doi.org/10.1021/ie303275e

Kazemian, M., & Shafei, B. (2023). Carbon sequestration and storage in concrete: A state-of-the-art review of compositions, methods, and developments. In *Journal of CO2 Utilization* (Vol. 70). Elsevier Ltd. https://doi.org/10.1016/j.jcou.2023.102443

Khan, S. A., & Koç, M. (2023). Buildability Analysis of 3D Concrete Printing Process: A Parametric Study Using Design of Experiment Approach. *Processes*, *11*(3). https://doi.org/10.3390/pr11030782

Kim, G. H., & Yang, J. W. (2025). Research trends in CO2 utilization: Catalytic strategies for sustainable energy and environmental protection. *Journal of CO2 Utilization*, *101*, 103216. https://doi.org/10.1016/j.jcou.2025.103216

Kim, N., Park, J., Amr, I. T., Bae, J. H., Fadhel, B. A., Cho, A., Tay, S. Y., Seo, J., & Lee, H. K. (2023). Hydration kinetics of ordinary Portland cement mixed under a direct CO2 inject condition. *Journal of Building Engineering*, *77*. https://doi.org/10.1016/j.jobe.2023.107531

Kmentová, H., Filip Edelmannová, M., Baďura, Z., Zbořil, R., Obalová, L., Kment, Š., & Kočí, K. (2025). Tuning CO2 reduction selectivity via structural doping of TiO2 photocatalysts. *Journal of CO2 Utilization*, *91*. https://doi.org/10.1016/j.jcou.2024.103008

Kristombu Baduge, S., Navaratnam, S., Abu-Zidan, Y., McCormack, T., Nguyen, K., Mendis, P., Zhang, G., & Aye, L. (2021). Improving performance of additive manufactured (3D printed) concrete: A review on material mix design, processing, interlayer bonding, and reinforcing methods. In *Structures* (Vol. 29, pp. 1597–1609). Elsevier Ltd. https://doi.org/10.1016/j.istruc.2020.12.061

Krstulovic, R., & Dabic, P. (n.d.). *A conceptual model of the cement hydration process*.

Lachmayer, L., Dittrich, L., Recker, T., Dörrie[2], R., Kloft[2], H., & Raatz, A. (n.d.). *Inline image-based reinforcement detection for concrete additive manufacturing processes using a convolutional neural network*.

Lee, M. G., Wang, Y. C., Wang, W. C., Ciou, B. S., & Liu, T. Y. (2025). CO2 sequestration and mechanical properties of recycled concrete. *Results in Engineering*, *26*. https://doi.org/10.1016/j.rineng.2025.104855

Li, L., Hao, L., Li, X., Xiao, J., Zhang, S., & Poon, C. S. (2023a). Development of CO2-integrated 3D printing concrete. *Construction and Building Materials*, *409*. https://doi.org/10.1016/j.conbuildmat.2023.134233

Li, L., Hao, L., Li, X., Xiao, J., Zhang, S., & Poon, C. S. (2023b). Development of CO2-integrated 3D printing concrete. *Construction and Building Materials*, *409*. https://doi.org/10.1016/j.conbuildmat.2023.134233

Li, L., Hao, L., Li, X., Xiao, J., Zhang, S., & Poon, C. S. (2023c). Development of CO2-integrated 3D printing concrete. *Construction and Building Materials*, *409*. https://doi.org/10.1016/j.conbuildmat.2023.134233

Li, X. S., Li, L., & Zou, S. (2023). Developing Low-pH 3D Printing Concrete Using Solid Wastes. *Buildings*, *13*(2). https://doi.org/10.3390/buildings13020454

Liu, B., Qin, J., Shi, J., Jiang, J., Wu, X., & He, Z. (2021). New perspectives on utilization of CO2 sequestration technologies in cement-based materials. In *Construction and Building Materials* (Vol. 272). Elsevier Ltd. https://doi.org/10.1016/j.conbuildmat.2020.121660

Liu, Q., Tang, H., Chen, K., Peng, B., Sun, C., Singh, A., & Li, J. (2024). Utilizing CO2 to improve plastic shrinkage and mechanical properties of 3D printed mortar made with recycled fine aggregates. *Construction and Building Materials*, *433*. https://doi.org/10.1016/j.conbuildmat.2024.136546

Lu, J., Wang, Z., Su, S., Liu, H., Ma, Z., Ren, Q., Xu, K., Wang, Y., Hu, S., & Xiang, J. (2024). Single-step integrated CO2 absorption and mineralization using fly ash coupled mixed amine solution: Mineralization performance and reaction kinetics. *Energy*, *286*. https://doi.org/10.1016/j.energy.2023.129615

Meesaraganda, L. V. P., & Kazmi, M. A. (2025). Performance Enhancement of Concrete Produced with two-step CO2 Mineralization. *Iranian Journal of Science and Technology - Transactions of Civil Engineering*, *49*(2), 1259–1271. https://doi.org/10.1007/s40996-024-01492-9

Misyura, S. Y., & Donskoy, I. G. (2020). Dissociation kinetics of methane hydrate and CO2 hydrate for different granular composition. *Fuel*, *262*. https://doi.org/10.1016/j.fuel.2019.116614

Monkman, S., MacDonald, M., Hooton, R. D., & Sandberg, P. (2016a). Properties and durability of concrete produced using CO2 as an accelerating admixture. *Cement and Concrete Composites*, *74*, 218–224. https://doi.org/10.1016/j.cemconcomp.2016.10.007

Monkman, S., MacDonald, M., Hooton, R. D., & Sandberg, P. (2016b). Properties and durability of concrete produced using CO2 as an accelerating admixture. *Cement and Concrete Composites*, *74*, 218–224. https://doi.org/10.1016/j.cemconcomp.2016.10.007

Osman, A. I., Hefny, M., Abdel Maksoud, M. I. A., Elgarahy, A. M., & Rooney, D. W. (2021). Recent advances in carbon capture storage and utilisation technologies: a review. In *Environmental Chemistry Letters* (Vol. 19, Issue 2, pp. 797–849). Springer Science and Business Media Deutschland GmbH. https://doi.org/10.1007/s10311-020-01133-3

Pan, Z., Si, D., Tao, J., & Xiao, J. (2023). Compressive behavior of 3D printed concrete with different printing paths and concrete ages. *Case Studies in Construction Materials*, *18*. https://doi.org/10.1016/j.cscm.2023.e01949

Peng, L., Shen, P., Poon, C. S., Zhao, Y., & Wang, F. (2023). Development of carbon capture coating to improve the durability of concrete structures. *Cement and Concrete Research*, *168*. https://doi.org/10.1016/j.cemconres.2023.107154

Pivezhani, F., Roosta, H., Dashti, A., & Mazloumi, S. H. (2016). Investigation of CO2 hydrate formation conditions for determining the optimum CO2 storage rate and energy: Modeling and experimental study. *Energy*, *113*, 215–226. https://doi.org/10.1016/j.energy.2016.07.043

Possan, E., Felix, E. F., & Thomaz, W. A. (2016). CO2 uptake by carbonation of concrete during life cycle of building structures. *Journal of Building Pathology and Rehabilitation*, *1*(1). https://doi.org/10.1007/s41024-016-0010-9

Qu, R., Xie, W., Wei, W., Suo, H., & Qin, Y. (2025). Organoboron catalysts: From structural design to functional application in CO2 conversions. In *Journal of CO2 Utilization* (Vol. 101). Elsevier Ltd. https://doi.org/10.1016/j.jcou.2025.103212

Quah, T. K. N., Tay, Y. W. D., Lim, J. H., Tan, M. J., Wong, T. N., & Li, K. H. H. (2023). Concrete 3D Printing: Process Parameters for Process Control, Monitoring and Diagnosis in Automation and Construction. In *Mathematics* (Vol. 11, Issue 6). MDPI. https://doi.org/10.3390/math11061499

Rymeš, J., Cervenka, J., & Jendele, L. (2024, January 7). *Material Modelling And Simulation Of 3D Concrete Printing Process*. https://doi.org/10.21012/fc11.092346

Schöler, A., Lothenbach, B., Winnefeld, F., Haha, M. Ben, Zajac, M., & Ludwig, H. M. (2017). Early hydration of SCM-blended Portland cements: A pore solution and isothermal calorimetry study. *Cement and Concrete Research*, *93*, 71–82. https://doi.org/10.1016/j.cemconres.2016.11.013

Seifu, M. N., Bersisa, A., Moon, K. Y., Kim, G. M., Cho, J. S., & Park, S. (2023). Exploring reaction and carbonation products of calcium silicate cement. *Journal of CO2 Utilization*, *71*. https://doi.org/10.1016/j.jcou.2023.102471

Sodeifian, G., Bagheri, H., Masihpour, F., Rajaei, N., & Arbab Nooshabadi, M. (2025). Niclosamide piperazine solubility in supercritical CO2 green solvent: A comprehensive experimental and modeling investigation. *Journal of CO2 Utilization*, *91*. https://doi.org/10.1016/j.jcou.2024.102995

Sousanabadi Farahani, H., Hosseini Zadeh, A., Hu, J., Hawkins, C., & Kim, S. (2025). Carbonation reaction of recycled concrete aggregates (RCA): CO2 mass consumption under various treatment conditions. *Cleaner Materials*, *15*. https://doi.org/10.1016/j.clema.2025.100296

Sun, B., Zeng, Q., Wang, D., & Zhao, W. (2022). Sustainable 3D printed mortar with CO2 pretreated recycled fine aggregates. *Cement and Concrete Composites*, *134*. https://doi.org/10.1016/j.cemconcomp.2022.104800

Sun, J., Guo, Y., Meng, Y., Jia, R., Zhou, J., Gao, H., & Liu, J. (2025). Effects of silicate modulus and GBFS content on shrinkage of alkali-activated steel slag cementitious material. *Journal of CO2 Utilization*, *91*. https://doi.org/10.1016/j.jcou.2024.103015

Sun, J., Xiao, J., Li, Z., & Feng, X. (2021). Experimental study on the thermal performance of a 3D printed concrete prototype building. *Energy and Buildings*, *241*. https://doi.org/10.1016/j.enbuild.2021.110965

Tarhan, Y., & Şahin, R. (n.d.). *DEVELOPMENTS OF 3D CONCRETE PRINTING PROCESS*. https://www.researchgate.net/publication/333673859

Tay, Y. W. D., Lim, S. G., Phua, S. L. B., Tan, M. J., Fadhel, B. A., & Amr, I. T. (2023). Exploring carbon sequestration potential through 3D concrete printing. *Virtual and Physical Prototyping*, *18*(1). https://doi.org/10.1080/17452759.2023.2277347

Wang, D., Xiao, J., Sun, B., Zhang, S., & Poon, C. S. (2023a). Mechanical properties of 3D printed mortar cured by CO2. *Cement and Concrete Composites*, *139*. https://doi.org/10.1016/j.cemconcomp.2023.105009

Wang, D., Xiao, J., Sun, B., Zhang, S., & Poon, C. S. (2023b). Mechanical properties of 3D printed mortar cured by CO2. *Cement and Concrete Composites*, *139*. https://doi.org/10.1016/j.cemconcomp.2023.105009

Wang, W. C., Lee, M. G., Deng, J. L., Wang, Y. C., Chuo, S. F., Pei-Chi, H., & Jen-Wei, S. (2024). Study on carbon sequestration and CO2 mixing of fresh cement mortar. *Case Studies in Construction Materials*, *21*. https://doi.org/10.1016/j.cscm.2024.e03813

Wen, Z., Yao, Y., Luo, W., & Lei, X. (2021). Memory effect of CO2-hydrate formation in porous media. *Fuel*, *299*. https://doi.org/10.1016/j.fuel.2021.120922

Wolfs, R. J. M., & Suiker, A. S. J. (2019). Structural failure during extrusion-based 3D printing processes. *International Journal of Advanced Manufacturing Technology*, *104*(1–4), 565–584. https://doi.org/10.1007/s00170-019-03844-6

Wu, H., Ma, X., Wang, W., Li, N., Shou, Y., Jiang, P., Zhou, F., & Zhan, H. (2025). Evolution of properties and microstructure of recycled aggregate mortars containing rice husk biochar under CO2 curing. *Journal of CO2 Utilization*, *101*, 103221. https://doi.org/10.1016/j.jcou.2025.103221

Xiong, B., Nie, P., Liu, H., Li, X., Zhao, G., Cheng, X., Zheng, G., Yang, X., & Wang, L. (2024). Evaluation and optimization of micro-calcium carbonate modified 3D printed rubber crumb concrete. *Construction and Building Materials*, *443*. https://doi.org/10.1016/j.conbuildmat.2024.137824

Zajac, M., Skocek, J., Haha, M. Ben, & Deja, J. (2022). CO2 Mineralization Methods in Cement and Concrete Industry. In *Energies* (Vol. 15, Issue 10). MDPI. https://doi.org/10.3390/en15103597

Zhang, T. (2024). *3D CONCRETE PRINTING MATERIAL PREDICTION AND FLOW SIMULATION USING PHYSICS-INFORMED NEURAL NETWORK*.

Zhong, K., Huang, K., Liu, Z., Wang, F., & Hu, S. (2024). CO2-Driven Additive Manufacturing of Sustainable Steel Slag Mortars. *ACS Sustainable Chemistry and Engineering*, *12*(29), 10919–10932. https://doi.org/10.1021/acssuschemeng.4c03018

Zhu, X., Wang, T., Yi, Z., & Zhu, Z. (2024). Kinetics and structure analysis of CO2 mineralization for recycled concrete aggregate (RCA). *Journal of Cleaner Production*, *448*. https://doi.org/10.1016/j.jclepro.2024.141571

Žitek Makoter, T., Kotnik, P., Makoter, T., Knez, Ž., & Knez Marevci, M. (2025). Optimization of the supercritical extraction and decarboxylation process of industrial hemp. *Journal of CO2 Utilization*, *91*. https://doi.org/10.1016/j.jcou.2024.103007

Zou, S., Xiao, J., Duan, Z., Ding, T., & Hou, S. (2021). On rheology of mortar with recycled fine aggregate for 3D printing. *Construction and Building Materials*, *311*. https://doi.org/10.1016/j.conbuildmat.2021.125312

Appendix

- **Appendix A: Appendix A-Project Schedule**
- **Appendix B: PhD Thesis planner-Chirag Vijay Kumar**
- **Appendix C: Operating Windows & Test Plan**

Common CO_2 Curing Parameters: All experiments will use a controlled carbonation environment in line with accelerated curing practice. Target gas concentration is ≈10% CO_2 (by volume), with low (≈5%) and high (≈20%) dose bands to bracket effects. Relative humidity is maintained at 60–70% RH (target 65%±5%) and ambient temperature at ~25 °C to mimic standard accelerated-curing conditions. An infrared thermal camera continuously monitors specimen surface temperature; the run is auto aborted if surface ΔT exceeds ~5 °C above baseline (approximately >30 °C absolute) to prevent thermal cracking or "chalky" carbonation layers. CO_2 exposure durations are selected based on mix and scale: for in-mix carbonation, 30–180 seconds of sealed contact in the mixer (per batch); for chamber curing of printed parts, typical periods of ~12, 24, and 36 hours will be tested. These windows reflect practical limits where benefits plateau and over-carbonation risks (microcracking, pore blockage) must be avoided.

Equipment & Nozzle Specifications: A gantry-style 3D printer with a progressive cavity pump will extrude the mortar through a 20 mm diameter nozzle (square profile). This nozzle size is chosen per literature on printable mortars (sand < 2 mm) to ensure consistent bead geometry. The printer enclosure will be shrouded with a clear plastic tent to serve as a curing chamber for post-print CO_2 exposure. Gas is introduced either by sublimating pre-weighed dry-ice pellets (solid CO_2) or via a mass-flow-controlled inlet for gas, depending on stage: in Phase 1 (mix-level dosing), crushed dry ice is added directly into the mixer at the start of mixing (lid immediately secured); in Phase 2 (early-age curing), gaseous CO_2 is released into the tent around the fresh print. In all cases, electronic sensors log CO_2%, temperature, and RH in real-time inside the chamber or mixer. A ppm CO_2 sensor with alarm is also placed in the lab to warn if any leak causes ambient levels >0.5% (5000 ppm) for safety.

Replication & Controls: Each test condition will be run with at least 3 specimens (n = 3) to ensure statistical reliability. Results will be reported as mean ± standard deviation for properties like strength, sorption, etc. All CO_2-treated batches have two reference counterparts cured concurrently: (1) a conventional cast control (no printing, no CO_2) to benchmark material performance, and (2) a printed control (printed identically but with no CO_2 exposure) to isolate the effect of carbonation. Performance metrics must meet minimum acceptance thresholds: no CO_2-treated sample should underperform the non-CO_2 printed control in any structural or durability metric. In practice, this means the printed CO_2 samples must match or exceed control compressive strength, have no interlayer bond reduction relative to non-CO_2 prints, and show equal or lower absorption/chloride penetration than controls. Any schedule that produces visible flaws (e.g. surface powdering, new cracks, layer delamination) or causes a drop in strength or durability below control will be flagged as unacceptable. Those parameters will be adjusted or eliminated in subsequent iterations. By enforcing these criteria – along with the real-time sensor cut-offs for temperature and humidity – the operating window for "safe and effective" CO_2 curing will be systematically narrowed down.

Planned Measurements: For each curing schedule, early-age properties (e.g. 1 day and 3 days compressive strength, 3-hour ultrasonic pulse velocity gain) will be measured to capture the immediate effects of CO_2. Buildability metrics (e.g. maximum unsupported layer count, achieved layer height vs. target) will document print quality under each condition. Hardened performance at 28 days will include compressive strength, interlayer tensile bond strength, four-point flexural strength (for printed beams), and transport properties (24 h water absorption, rapid chloride migration coefficient). Results will be tabulated as mean ± SD and compared against the control benchmarks. A successful CO_2 curing schedule is one that improves early stiffness/strength and/or durability without compromising print geometry or bond. As an additional acceptance gate, the project's carbon accounting will only credit CO_2 uptake from schedules that meet or exceed all control performance – this ensures no sustainability trade-off at the expense of quality.

- **Appendix D: CO_2 & Dry-Ice SOP + Safety Controls**

CO_2 Handling and Injection SOP: All carbonation curing will follow a strict protocol to ensure consistency and safety. For mix-phase carbonation (Phase 1), the procedure is: pre-weigh the required dry-ice (solid CO_2) dose in a vented container (wear cryogenic gloves and face shield), add it to the mixer immediately after water and before high-speed mixing, then clamp down the mixer lid with a foam gasket seal. The

dry ice will sublimate in the sealed mixer, providing the CO_2 dose for ~2–3 minutes of mixing. After the set contact time (monitored by a stopwatch and logged), the mixer is opened in a fume hood or well-ventilated area to release any excess CO_2 before retrieval of the fresh mix. Purge the mixer with fresh air for >1 min before an operator looks in. For early-age chamber curing (Phase 2 and 3), once a specimen or printed section is placed in the curing tent (an airtight plastic enclosure over the print bed), CO_2 gas from a cylinder is introduced through a regulator and diffuser. Gas flow is initiated at a low rate to displace air until reaching the target 10% concentration – verified by an in-tent CO_2 sensor. The tent or chamber is then sealed for the designated curing period. Humidity is maintained by placing a damp sponge or ultrasonic humidifier inside to target ~65% RH (to prevent the sample from drying out). Throughout exposure, an IR camera tracks surface temperature (see below), and periodic readings from the CO_2 and RH sensors are recorded in the log. After curing, the chamber is vented slowly (unzipped or unsealed in partial openings) in a fume-hood or outdoor area to avoid a surge of CO_2 into the lab.

Sensor Thresholds & Automation: A multi-channel data-logger will continuously monitor: (a) CO_2 concentration inside the curing enclosure, (b) relative humidity and temperature, and (c) specimen surface temperature via IR thermography. Thresholds are programmed such that if CO_2 exceeds the setpoint by >1% (absolute) or RH deviates outside 60–75%, the mass flow controller or humidifier will auto-adjust to compensate (or shut off CO_2 if out-of-range). Crucially, if the IR camera detects the specimen surface exceeding 30 °C (the thermal “cap” determined to prevent damage), an alarm triggers and the CO_2 inlet is shut off automatically. In practice, a sustained temperature rise of ~5 °C above ambient is treated as the cutoff for safety. At that point, fans will purge the chamber/tent with fresh air to cool the sample. Similarly, the appearance of a “chalky” white surface on the concrete (visual sign of over-carbonation) is grounds for immediate termination of that run – operators are trained to observe this through the clear tent walls. All sensor data (CO_2%, RH/T, IR temperature) are logged per second as part of the QA/QC record for each trial. These logs will be reviewed to ensure each test stayed within the intended window; any excursion (e.g. RH drop leading to drying) invalidates the test and it will be repeated after adjusting parameters.

Dry-Ice Feeding & Personal Safety: When handling dry ice for mix injection, small pellets (~10 mm size) are used for rapid sublimation. They are added to the mix only after all other ingredients are in and the mixer is about to be sealed – this minimizes open-air sublimation. The operator must wear insulated gloves, long sleeves, and a face shield (to guard against splinters of dry ice and intense cold). All observers stand clear during the initial seconds of mixing. If the mixer lid has a pressure relief, it will be checked to ensure it’s functioning (to vent excess gas and avoid overpressure). After the mixing period, the drum is opened cautiously and ventilated as described. Any solid CO_2 remaining (unlikely, as it will mostly have sublimated) is left to sublime in the hood – never sealed in a waste container. For the chamber curing, CO_2 cylinders are secured upright and equipped with a two-stage regulator and flow meter. Connections are leak-checked with a soap solution before each use. The flow rate is kept low (e.g. <2 L/min) during initial purge to prevent disturbing lightweight prints and to avoid over-pressurizing the tent. An oxygen depletion alarm is installed in the laboratory space: if ambient O_2 falls below 19.5% (indicating CO_2 buildup), audible and visual alarms will trigger, and the building HVAC will ramp up ventilation. Team members have been instructed in CO_2 safety: always work in pairs when entering an enclosed curing area and ventilate the space thoroughly before any close inspection of the specimens.

Safe Setup and Shutdown: Prior to each print or curing run, a safety checklist is followed. Key points: (1) Ventilation – lab exhaust fans on high, and doors open (if possible) when releasing CO_2. (2) No ignition sources – while CO_2 is non-flammable, the procedure avoids any confusion with pressurized gas handling protocols (standard compressed-gas safety applies). (3) Emergency stop – the CO_2 supply has a clearly labeled shut-off valve accessible outside the tent, and the printer power has an emergency cut-off in case of any abnormal event. After CO_2 curing, the concrete specimens are moved to ambient curing or water curing as needed. The chamber tent is purged with fresh air (fans blowing in) for several minutes before opening fully. DO NOT enter an enclosed cure chamber immediately after high-CO_2 curing – the area is first tested with a handheld CO_2 meter to ensure levels are back to near normal (<0.5%). Finally, all gas cylinders are closed at the main valve after use, and pressure in regulators bled off. Any ice or condensate on equipment (from cold CO_2 expansion) is wiped dry to prevent slip hazards. By adhering to these SOPs, the team ensures that the innovative use of CO_2 in printing poses minimal risk to personnel and facilities while maintaining full control over the curing process.

- **Appendix E : LCA Assumptions & Calculation Log**

System Boundary & Declared Unit: The life-cycle assessment will be cradle-to-gate, encompassing raw material production (cement, aggregates, admixtures), mix preparation and printing, and the CO_2 curing process up to the point the element is ready for use. The declared unit is 1 m³ of 3D-printed concrete (structural element) cured under the new CO_2 process, as this provides a functional basis to compare against 1 m³ of conventionally cured printed concrete. All inputs and outputs are tracked per cubic meter. The boundary includes cement manufacture (with its clinker factor and associated CO_2 emissions), production of SCMs (e.g. calcination energy for metakaolin if used), aggregate mining and transportation, mixing energy, and CO_2 capture and delivery. It stops at the factory gate – so downstream aspects like use-phase and end-of-life are excluded (though a carbonate stability assumption is noted for end-of-life). By focusing cradle-to-gate, we capture the embodied carbon and the immediate impact of CO_2 curing on that footprint.

CO_2 Source, Capture, and Transport Assumptions: We assume the CO_2 used for curing is sourced from an industrial waste stream (e.g. a fertilizer plant) and would otherwise be emitted to atmosphere – thus the CO_2 itself is treated as having zero “biogenic” or anthropogenic emission cost (i.e. we don’t count its chemistry as new carbon). However, the energy required to capture, liquefy, and transport that CO_2 is included. For a baseline, we use an estimate of 0.1–0.2 kWh of electricity per kg CO_2 for compression and cooling (assuming bulk CO_2 supply) and a trucking distance of 100 km in insulated cylinders. These inputs add a small carbon penalty per kg CO_2 used, which is accounted for. In one scenario, we will also examine direct air capture (DAC) CO_2 (which has a very high energy cost ~1 kWh/kg CO_2) just for sensitivity, although it’s not the primary source. It’s assumed CO_2 curing uses approximately 5–15 kg CO_2 per m³ concrete (depending on the dose band: low, mid, high). For each test, the exact CO_2 consumed (mineralized) is measured via mass gain/TGA, and any excess CO_2 vented is not counted as sequestered. Transportation of CO_2 is modeled using a diesel truck (ton-km) factor for the cylinder delivery. All these assumptions are logged in the LCA calculation spreadsheet (“CO2_LCA_Log.xlsx”) for transparency.

Mix Design and Production Inputs: The concrete mix is a Portland-limestone cement (PLC) based mortar with typical 3DCP admixtures. We model cement impacts using EPD data for CSA GU or Type IL cement (with ~10% limestone) adjusted for our clinker content. If SCMs are used (e.g. slag or fly ash), their “upstream” burdens are included (slag assumed to carry the grinding energy and a small allocation from blast furnace, fly ash is treated as industrial byproduct with minimal burden, aside from processing). Superplasticizer and other additives are included at their production impact per kg. Mixing energy is based on the electrical energy of our mixer and pump during a print (monitored via a power meter – roughly on the order of 5–10 kWh per m³, which is small but counted). The printing process (robot motion) electricity is also included (estimated from machine specs). These are summed in the cradle-to-gate inventory.

Carbonation Curing Process in LCA: The CO_2 curing itself has two opposite contributions in the carbon balance. On the emissions side, we include any energy for CO_2 curing (e.g. the IR heating or humidification if used, any fans, sensors – though minor, we include them for completeness). On the savings side, we credit the CO_2 sequestered permanently in the concrete. Following ISO <small>21930</small> and EN 15804 guidelines, we can subtract the amount of CO_2 mineralized in the product from the net GHG emissions of that product, provided it is expected to remain locked for the building’s life (100+ years). In our case, CO_2 is stored as thermodynamically stable calcium carbonates (calcite/aragonite) in the hardened matrix, which will not re-emit under normal use. Thus, we apply a negative CO_2 emission for the kilograms of CO_2 uptake measured (e.g. if 10 kg CO_2 are stored per m³, that’s –10 kg CO_2 in the emission tally for that scenario). However, we will also run a sensitivity where, if the element is demolished and crushed, some fraction of carbonates might re-carbonate or release CO_2 over end-of-life (e.g. in an acidic environment). For now, the base assumption is full permanent storage (100% credit) as a conservative stance in line with other carbonation cure studies. The LCA log will clearly state the credited CO_2 amount and any assumed timing (we assume the credit at the moment of curing, since that’s within the system boundary of cradle-to-gate for storage).

Credits and Co-product Allocation: No co-products are produced in our system except the primary concrete element. If any material savings occur (for instance, if CO_2 curing allows a lower cement content for the same strength – a hypothesis to test), we would account for that by reducing cement input for equivalent performance. That kind of improvement would appear as a reduced impact in the CO_2-cured mix scenario. We do not generate excess energy or reusable byproducts to credit. The only “credit” comes from the carbon sequestration in the product itself (sometimes termed negative emissions or carbon storage). We will ensure to follow the ILCD/EN 15804 rules for declaring stored carbon: it will

be reported separately in the LCA results (as kg CO_2 sequestered). If the print has reinforcement (none in Phase 1–2 tests, but possibly steel fibers in Phase 3 element), the additional emissions for steel (and any change in its production due to CO_2 curing effects, likely none) are included as well.

LCA Calculation Log: All calculations are documented in a stepwise fashion in the provided Excel log. For each mix design and curing schedule, the log shows raw material quantities (kg), their embodied CO_2 from databases, process energy inputs (MJ or kWh converted to CO_2 using regional electricity factors), transportation distances, and finally the CO_2 uptake credit. Intermediate values like "effective CO_2 curing energy per m³" and "CO_2 cured concrete net CO_2" are shown. The log also includes a segment for same-schedule comparison, meaning we align the age at testing for fair comparison (since our claim is carbon curing doesn't sacrifice performance, we ensure we're comparing equal-strength designs or same curing durations). The cradle-to-gate global warming potential (GWP) is the primary indicator, though we will also note if there are changes in other indicators (e.g. if CO_2 curing eliminates the need for steam curing, we also credit the avoided steam energy and its emissions). For instance, if a steam-cured reference uses 5 kWh of heat per m³, the CO_2-cured version avoids that – we include that avoidance as well. Such assumptions are clearly annotated in the log file.

The LCA assumes a fair accounting where any extra emissions for implementing CO_2 curing (gas production, transport, power) are added, and any carbon stored, or energy saved are subtracted. The goal is to truthfully compute the net carbon footprint per unit of CO_2-cured printed concrete, ensuring that we only claim a **"carbon-negative" or "carbon-saving" outcome if the math (within these boundaries) supports it. The detailed assumptions and calculations will be available for review in Appendix tables, and key results will be used to support the feasibility of the process in the proposal.

- **Appendix F: Calibration & Threshold Pack**
  - **UPV to early-age stiffness and print timing**

Purpose. Use UPV only as a timing beacon so we deposit layers at the right stiffness. We do not claim UPV equals strength. Strength is still from tests.

Specimens and schedule. Make small cubes or cylinders from the same batch you will print. Take UPV at about 3 hours, 6 hours, 9 hours, and 24 hours. At 24 hours, test companion pieces in compression so the curve is anchored to a real point.

How we build our curve.

1. Set up the UPV probes the same way every time. Use the same couplant. Wipe surfaces clean.
2. Record at least three readings per time point and keep the average.
3. Plot UPV against time on one page. Add your 24-hour strength point on the same sheet for reference.
4. Keep the smooth curve that fits the points well. If one point looks wrong, repeat it once and keep the median of the three tries.

How we turn this into print timing.

- Run one or two small bench prints and note the time (or UPV) when the bead holds shape, does not slump after 15–30 minutes, and still bonds well to the next layer.
- Mark this as your **print timing band** (for example: "print when UPV is roughly between X and Y" or "print between 50 and 80 minutes after batching" if that is more practical).
- Write this band on the day's build card. During runs, if we are **below** the band we wait; if we are **above** the band we shorten layer height or stop, because bond can suffer when we print too late.

What we store. The one-page UPV curve with the timing band, the raw readings, date, mix ID, and who took the readings. Put the PDF or image in the run folder.

  - **ATR-IR and TGA "pass" thresholds for carbonation**

Purpose. Make a simple pass call from spectra and thermogravimetry so we do not promote a schedule that is under-carbonated or over-carbonated.

Sampling.

Early screen at about 2 hours: take a thin surface sample (2–3 mm).

Decision point at about 24 hours: take both a surface sample and a mid-depth sample.

ATR-IR pass rules.

At about 2 hours, the strong carbonate band near 1410 to 1470 should be clearly visible and not “faint”. If it is faint, we hold or re-run.

At about 24 hours, the carbonate band is strong at mid-depth and does not jump much compared with the 2-hour check. This means we are close to a plateau, not only a skin effect.

TGA pass rules.

At about 24 hours, the portlandite loss band is small. That means most portlandite has reacted.

At about 24 hours, the carbonate loss band is present and not marginal. As a rough anchor, the carbonate mass loss should be at least a couple of percent of binder, or clearly above the control.

Promote, hold, drop.

Promote when both ATR-IR and TGA look right and there is no chalky surface and no new microcracking.

Hold when ATR-IR looks good, but TGA is only just there. Re-check once. If still weak, reduce dose or contact time and try again.

Drop when ATR-IR stays weak at 24 hours, when portlandite is still clearly present, or when a chalky skin appears.

What we store. A single-page report with the two ATR-IR screenshots (surface and mid-depth) and the TGA curve with the bands highlighted, plus the sampling photos.

- **Short RCPT surrogate and how we keep it honest**

Purpose. Use a quick transport indicator at early age, but only when we have proof it tracks the full test.

How we prove it.

Pick six to eight mixes from your past work, including at least one slag-rich and two printable mortars.

For each, plot the short test value against the proper migration or RCPT value measured at the standard age.

Keep the simple best-fit line with a clear plot and the error written on the page in words (for example: “the short test predicts the standard within about ten percent inside this range”).

Where we use it.

In Micro and Meso stages we report the short test as percent change versus the printable control on the same day.

In Macro we use the short test only when the result lies inside the proven range. If it is outside the range, we run the standard test.

What we store. One page with the scatter plot and the simple sentence about the fit quality. A short table that lists the mixes and their values.

- **Sensors, alarms, and how we prevent drift**

Set-up. We use a CO_2 sensor in the tent, a second CO_2 or oxygen alarm in the lab for safety, a combined humidity and air temperature sensor in the tent, and an infrared camera on the specimen surface. We log at one reading per second and save the CSV file in the run folder. We take a photo of the infrared screen at the highest temperature during the run and save it in the folder.

Emissivity for the infrared camera. Place a small matte tape patch near the region of interest and set the camera so the concrete and the tape read the same number. Keep this setting for the day.

Alarms and caps.

CO_2 inside the tent holds near ten percent. Alarms if it falls well below or rises well above that band.

Humidity stays near the mid-sixties. Alarms if it drops below the high fifties or goes above the mid-seventies.

Surface temperature should not climb more than a few degrees above room temperature and not exceed about thirty degrees overall. If it does, we stop gas, vent the tent, and log the cause.

If any sensor drifts or freezes, we void the run, fix the sensor, and repeat. The voided log stays in the folder with “sensor drift” noted.

What we store. One page with the graph of CO_2, humidity, and temperature over time, the infrared photo at peak, and the checklist with all boxes ticked or crossed.

- **Ready-to-use forms (what each page will contain)**

Print and cure log (per run). Specimen ID, date and time, mix ID, dry-ice dose, contact time, tent CO_2 (if used), humidity and air temperature, infrared peak temperature, any abort, short note on what changed.

Geometry and buildability. Target bead width and height, measured values at placement and at 15–30 minutes, wall target height, achieved height, failure mode if any (buckle, slide, collapse), a box for “pass” or “repeat”.

Interlayer bond. Specimen ID, test type (pull-off or slant-shear), test area or coupon size, peak load or stress, failure mode (glue, substrate, or interface), ratio versus printable control, a box for “pass” or “repeat”. Glue or substrate failures do not count as bond results.

Durability mini-panel. Absorption at 24 hours, transport value from the short test, carbonation depth check if used, all reported as less than or equal to the printable control, a box for “pass” or “repeat”.

Pass sheet. Geometry pass, bond pass, durability pass, no chalking, infrared cap respected, sensors within bands, sign-off by tester and witness.

- **Dry-ice safety and best practice (primary route)**

Before you start. Wear cryogenic gloves, eye and face protection, long sleeves. Weigh pellets quickly and keep them in an open tray so gas can vent. Seal the mixer lid before the pellets fully sublimate. Stand clear for the first seconds of mixing.

After mixing. Open the mixer in a fume hood or a space with strong air flow. Let gas clear before anyone looks inside. Do not trap dry ice in a closed bin. Let it fade in the hood.

For prints with a tent. Use low and steady gas flow so filaments are not disturbed. Keep humidity stable. Never climb inside a tent full of CO_2. Always vent and verify safe air before any close work.

- **Quality check points in plain words**

1. We only move a schedule forward when the bead and wall stay within the target size band and the wall reaches target height without a failure.
2. We only move a schedule forward when interlayer bond is the same as the printable control or higher.
3. We only move a schedule forward when the absorption and the transport indicator are the same as the printable control or better.
4. We stop and adjust if we see chalking, if the surface overheats, or if sensors go out of band.
5. We only claim carbon credit when the element passes all of the above and we have measured storage from ATR-IR and TGA for that schedule.